

# Chapter 16

## Establishing the Links Between A $\beta$ Aggregation and Cytotoxicity In Vitro Using Biophysical Approaches

Asad Jan and Hilal A. Lashuel

### Abstract

Aggregation and fibril formation of the amyloid- $\beta$  (A $\beta$ ) peptides play a pivotal role in the pathogenesis of Alzheimer's disease (AD). The missing links on the pathway to A $\beta$  oligomerization, fibril formation, and neurotoxicity in AD remain the identity of the toxic A $\beta$  species and mechanism(s) of their toxicity. Such information is crucial for the development of mechanism-based therapeutics to treat AD and tools to diagnose and/or monitor the disease progression. Herein, we describe a simple approach that combines standard biophysical methods with cell biology assays to correlate the aggregation state of A $\beta$  peptides with their cytotoxicity in vitro. The individual assays are well-established, commonly used, rely on easily accessible materials and can be performed within 24 h.

**Key words:** Alzheimer's disease, Amyloid- $\beta$ , Oligomers, Toxicity

---

### 1. Introduction

Alzheimer's disease (AD) is the most common cause of debilitating dementia in elderly worldwide. Despite significant advances in the understanding of the mechanisms of A $\beta$  production and aggregation in vitro, translating this knowledge in a clear mechanistic understanding of the pathogenesis of AD and effective clinical therapies remain challenging. Circumstantial evidence, principally derived from neuropathology, molecular genetics, animal models of AD, cell culture studies, and biophysics indicate that the aggregation and fibril formation of amyloid- $\beta$  (A $\beta$ ) peptides play central role in AD pathogenesis (1, 2). A $\beta$  peptides are produced as a consequence of sequential proteolytic processing of the amyloid precursor protein (APP) by  $\beta$ - and  $\gamma$ -secretase activities. APP cleavage by  $\gamma$ -secretase results in production of A $\beta$  peptides of various chain lengths, principally composed of 40 and 42 amino acid

residues (A $\beta$ 40 and A $\beta$ 42), which densely populate the core of the neuritic plaques in AD neuropathology (3). During the *in vitro* fibril formation of A $\beta$  peptides, various nonfibrillar aggregates of diverse morphologies and heterogeneous size distributions, collectively known as the soluble oligomers, have been observed. Some of the well-characterized A $\beta$  oligomer species include protofibrils (4), A $\beta$ -derived diffusible ligands (ADDLs) (5), annular oligomers (6), and the low molecular weight oligomers (7).

Several independent lines of evidence indicate that the soluble oligomers and/or the process of oligomerization (8–10), rather than plaque-associated fibrils, are the primary cause of neurodegeneration in AD: (1) Soluble A $\beta$ , rather than total (soluble and insoluble) A $\beta$ , levels correlate better with AD progression (11, 12); (2) Significant functional deficits in the memory performance tasks are observed in the APP transgenic animals long before the emergence of amyloid plaques (13, 14); (3) Soluble A $\beta$  oligomer preparations, upon intracerebral infusion, induce transient memory deficits in experimental animals (15); (4) Rare mutations in the APP gene [e.g., arctic mutation (E22G)], which enhance A $\beta$  oligomerization without altering the total A $\beta$  levels, are associated with the development of familial AD (16); (5) A $\beta$  oligomer and protofibril preparations alter neuronal metabolism (17), induce changes in neuronal electrophysiology (18) and lead to neurotoxicity towards cultured neurons (10, 17, 19). Therefore, inhibiting A $\beta$  oligomerization, by attenuating its production and/or promoting the clearance of toxic A $\beta$  oligomers from brain, has emerged as potential therapeutic strategies for treating AD (20).

Cultured primary neurons and/or cell lines provide easy and economic means of investigating the role of A $\beta$  aggregation state and the mechanism of A $\beta$  toxicity, and also as valuable tools for the screening of the inhibitors of A $\beta$  toxicity *in vitro*. This chapter describes simple, inexpensive, and reproducible methods which would allow the investigators to assess the toxicity of A $\beta$  preparations (soluble or insoluble) and correlating A $\beta$  aggregation/fibrillization with its cytotoxicity. The general outline is provided in Fig. 1. Briefly, cultured cells are treated with purified A $\beta$  preparations (monomers, protofibrils, and fibrils) or crude preparations containing mixtures of heterogeneous A $\beta$  species. For detailed protocols on the preparation of these species, the reader is referred to our previous work (10, 21). At desired intervals, cell viability is determined by the MTT (3-(4,5-dimethylthiazol-2-yl)-2,5-diphenyltetrazolium bromide) reduction assay. In the case of primary neurons, subtle changes in neuronal viability can also be quantified using immunostaining for neuronal nuclei (NeuN) (8) or via quantification of the loss of neuronal processes (19, 21). In addition, media aliquots of A $\beta$ -treated cultured cells can be used to investigate the cytotoxicity and the aggregation state of A $\beta$  simultaneously. Quantitative cytotoxicity information can be obtained by performing

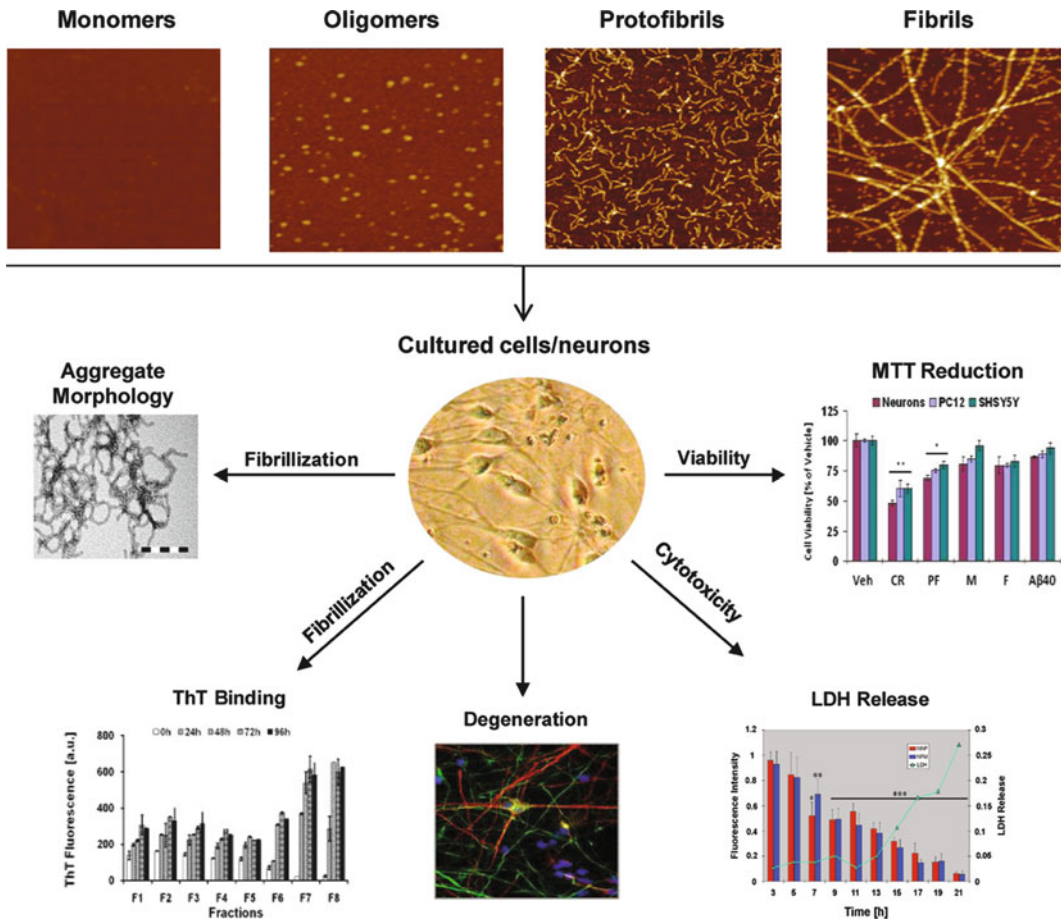


Fig. 1. Overview of the methods used to correlate A $\beta$  aggregation with cytotoxicity in vitro. Cultured cells (primary neurons and/or cell lines) are treated with the desired concentration(s) of the purified or crude A $\beta$  preparations (21). At selected intervals, cell viability can be assessed by the MTT reduction assay. In the case of neuronal cultures, immunostaining for neuronal nuclei (NeuN) (8) or neuronal processes (19) can also be used. The culture medium can be assayed for cytotoxicity using the LDH release method. In addition, A $\beta$  aggregation and fibrillization can be monitored by ThT dye binding and TEM analysis of the culture medium and allow for the correlation of the A $\beta$  aggregation with the relative cytotoxicity (the MTT graph and the LDH release graphs are reprinted with copyright permission (10, 19)). Labels in the MTT graph: cultured primary neurons, PC12 and SHSY5Y cells were treated with different A $\beta$  preparations (10  $\mu$ M total A $\beta$ ) or the buffer vehicle and cell viability was assessed by the MTT reduction assay (*Veh* buffer vehicle, *CR* crude A $\beta$ 42 preparations, *PF* A $\beta$ 42 protofibrils, *M* A $\beta$ 42 monomers, *A $\beta$ 40* A $\beta$ 40 monomers) (10). Labels in the LDH graph: cultured primary neurons were treated with A $\beta$ 40-arctic (E22G) monomers (20  $\mu$ M total A $\beta$ ) and cell viability was assessed over time by the LDH release in the culture medium and quantitative immunocytochemistry for the microtubule-associated protein (MAP) and neurofilament-M (NF-M) (19).

the lactate dehydrogenase (LDH) release assay using the cell culture medium. Finally, a direct link between the extent of cytotoxicity and A $\beta$  aggregation state can be established by combining these assays with methods that allow monitoring of A $\beta$  aggregation in the cultured media, e.g., dye [Thioflavin T (ThT)] binding and negative-staining transmission electron microscopy (TEM).

This approach will allow the researchers to closely monitor changes in the quaternary structure of A $\beta$  under cell culture

conditions, formation of oligomers and fibrils during the duration of the experiment, and most importantly, directly correlate A $\beta$  aggregation state(s) with relative cytotoxicity. The knowledge gathered from such studies is indispensable for the identification of the critical stages (aggregation states) on the A $\beta$  amyloid formation pathway which underlie A $\beta$  cytotoxicity and help design the intervention strategies. Herein, we describe the use of MTT reduction and the LDH release assays for quantifying A $\beta$  toxicity toward cultured PC12 cells. Detailed methods for culturing primary neurons, including immunostaining and measuring cell viability by relevant assays, have been described elsewhere (8, 21).

### 1.1. MTT Reduction Assay

MTT [3-(4,5-dimethylthiazol-2-yl)-2,5-diphenyltetrazolium bromide] belongs to the group of tetrazolium salts which, upon endocytosis by the cells, is reduced to the insoluble formazan crystals principally by the activity of the mitochondrial respiratory chain enzymes (22). In addition, certain enzymes in cytoplasm, endosomes/lysosomes, and plasma membrane have also been implicated in the metabolism of MTT into the formazan (23). Metabolically active and viable cells can reduce the MTT in short durations of time, e.g., 30 min, into purple formazan products the formation of which can be monitored spectrophotometrically (Fig. 2) (23). It is one of the most commonly used assays to monitor cytotoxicity of various drugs, synthetic polymers, and amyloid proteins (17, 24, 25). Numerous research groups have shown that A $\beta$  preparations containing monomers, oligomers, or fibrils consistently impair the ability of cultured neurons or other cells to metabolize MTT (9, 17, 26). The simple nature of the assay and

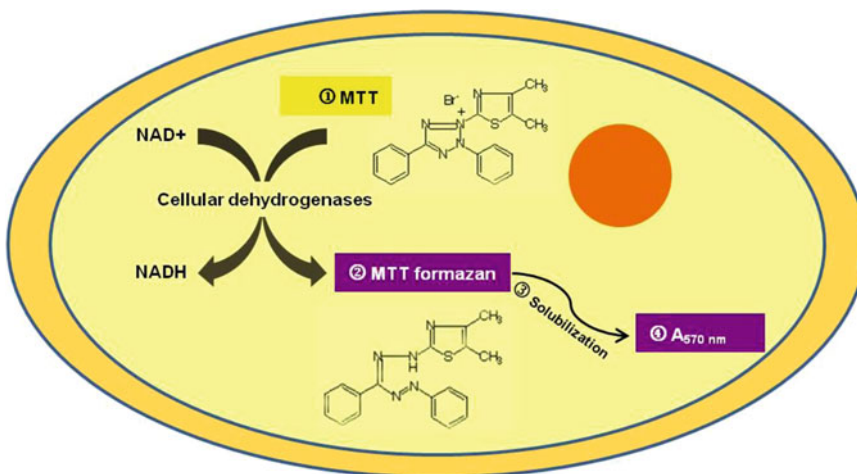


Fig. 2. Principle of the MTT assay. MTT is internalized by the cells and reduced by the action of various cellular dehydrogenases, principally in mitochondria, into the purple formazan product. The crystals of formazan are solubilized and the absorbance (570 nm) of the resulting solution provides a measure of the cellular viability.

the lack of requirements for expensive instrumentation make it a convenient choice for assessing the relative toxicity of A $\beta$  preparations and also for the evaluation of the A $\beta$  aggregation inhibitors in rescuing the survival of A $\beta$ -treated cells.

Although it is very easy to perform, some shortcomings of the assay are worth mentioning: (1) the assay does not differentiate between cell death and metabolic stress (27); (2) the readout is semiquantitative, i.e., a decrease in MTT reduction does not correlate with number of dead cells in a linear fashion (27); (3) different cell types metabolize MTT, and related tetrazolium dyes, to differential extent, i.e., the assay readout is influenced by the metabolic phenotype of the cells (28); and (4) it has also been suggested that amyloidogenic proteins interfere with crystallization of MTT formazan in a manner such that the extent of cytotoxicity is overestimated (9). Therefore, it is highly recommended that MTT reduction assay be used in conjunction with some other biochemical and/or immunocytochemical means of assessing the cell viability, e.g., LDH release assay (see below) and/or, in the case of neurons, staining for the loss of neuronal processes.

### 1.2. LDH Release Assay

LDH is an oxidoreductase enzyme present in the cytoplasm of a wide variety of cells and catalyzes the interconversion of pyruvate and lactate, coupled to the concomitant interconversion of NADH and NAD<sup>+</sup> (29, 30). Cell membrane disruption, during various physiological or pathological processes, leads to the release of the enzyme in extracellular milieu (e.g., cell culture medium). Hence, if appropriate substrates are added to the culture medium, the levels of LDH release, and therefore the extent of cell membrane damage, can be quantified (Fig. 3). LDH release is also a commonly used assay for investigating the biosafety of drugs and for assessing the cytotoxicity of the amyloidogenic proteins including A $\beta$  (31, 32).

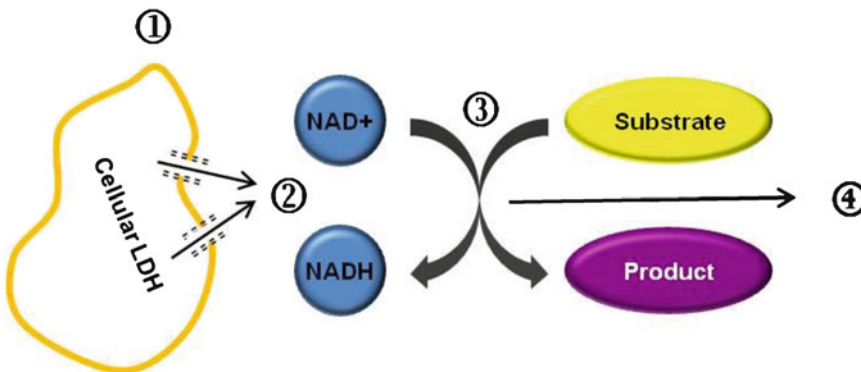


Fig. 3. Principle of the LDH release assay. Upon ① membrane disruption/cell damage, ② the cytosolic LDH is released into the extracellular milieu/tissue culture medium. In the presence of appropriate substrates and cofactors, ③ the enzyme activity results in ④ the formation of colorimetric/fluorescent products. The latter can be quantified and indicate the extent of cytotoxicity.

Interestingly, it has been observed that in neuronal cultures exposed to A $\beta$  oligomers, loss of neuronal processes precedes the rise in LDH release. The latter observations suggest that A $\beta$  oligomer toxicity is mediated by multiple mechanisms and the neurodegeneration commences long before the frank death of neurons (9, 10, 18, 19).

In contrast to the MTT reduction assay, the amount of LDH release provides a more reliable measure of the number of dead/damaged cells (33). However, it is also known that different cell types have differential LDH content and/or the kinetics of the LDH release is not identical (34); therefore, correlation of the assay readout to the extent of cell death between different cell types cannot be accurately determined. Nevertheless, the combined application of the two assays (MTT and LDH) provides valuable information regarding both the early and the late events associated with A $\beta$  cytotoxicity.

### **1.3. Negative-Staining TEM**

Electron microscopy (EM)-based approaches have played important role in our current understanding of the mechanism of amyloid formation of nearly all amyloidogenic proteins, and also in elucidating the structural basis of amyloid toxicity. As early as 1960s, these approaches facilitated the detailed structural characterization of amyloid aggregates associated with neuropathological lesions in AD brains (35). In addition, EM methods have also played important role in the discovery and structural characterization of various A $\beta$  oligomers, including protofibrils, which precede the emergence of fibrils during the aggregation of A $\beta$  peptides (4, 17). The latter findings significantly changed the paradigm of understanding the interrelation of the process of amyloid formation and associated neurodegeneration, and ushered the notion of toxic oligomer/protofibril hypothesis (36). Although, the toxicity of plaque-associated fibrillar aggregates is not ruled out, this hypothesis points toward soluble A $\beta$  oligomers as neurotoxins in AD and stipulates that the A $\beta$  oligomers trigger a complex series of the cellular and molecular events culminating in the development of AD (36). A detailed description of various EM-based methods and their utility in studying amyloid aggregation can be found elsewhere (21, 37).

Herein, we describe the methods and use of the negative-staining EM on the cell culture media aliquots to study A $\beta$  aggregation under cell culture conditions, and directly establish the correlation of the aggregate structure with their respective cytotoxicity in neuronal and nonneuronal cell culture systems. In brief, cell culture medium aliquots are deposited on carbon-coated formvar film attached to an EM grid, followed by the staining with a dilute solution of a heavy salt (uranyl acetate, uranyl formate etc.). The latter help enhance the contrast in the images by their ability to scatter electrons in the incident electron beam. Although, a convenient and simple method, the quality of the information obtained by negative-staining EM is limited by certain factors such as: (1) limited resolution capability ( $\approx 2.5$  nm) of the technique, (2) drying of the

surface causes flattening of the aggregate structures, (3) the aggregates may differ in their adsorption to the grid surface, (4) image artifacts can be induced by uneven staining of the sample (this could be addressed by preparing multiple grids of the sample), and (5) most importantly, it is not a quantitative method. Therefore, it is suggested that information about the characterization of amyloid aggregates should be complimented by other standard biophysical assays, e.g., Thioflavin-T (ThT) dye binding and solubility analysis by the size exclusion chromatography (6, 8).

#### **1.4. Thioflavin-T Dye Binding**

Thioflavin-T (4-(3,6-dimethyl-1,3-benzothiazol-3-ium-2-yl)-*N,N*-dimethylaniline chloride), and its homologue Thioflavin-S, is a benzothiazole salt and belongs to the so-called amyloid-specific dyes. The thioflavin dyes undergo red shift in their emission spectrum upon binding to amyloid plaques in amyloid laden tissue sections (38, 39). In vitro, thioflavin dyes bind to the ordered amyloid aggregates such as fibrils and protofibrils of diverse proteins, e.g., A $\beta$  (8, 17),  $\alpha$ -synuclein (40), but not to the low molecular weight oligomers (2–12 mers) or monomers (8, 17). The specificity of the dyes for binding to the amyloid structures has been proposed to be based on the presence of the cross-strand ladders, characteristic arrangements of side chains, present in  $\beta$ -sheet-rich structures, and formation of channels along the  $\beta$ -sheet surfaces which allow for the binding of linear thioflavin dyes (Fig. 4) (41). Although very simple and inexpensive method, ThT binding per se does not always provide a quantitative measure of the amount of amyloid aggregates, e.g., a small amount of fibrils in A $\beta$  preparations can result in high-ThT values. Also, extensive fibrillization, and intertwining of the fibrils, may reduce the accessibility of ThT dyes towards the binding sites thus erroneously decreasing the ThT readout. Nevertheless, changes in ThT binding in kinetic assays is a reliable indicator of the metastability in amyloid aggregates and, if used in combination with cytotoxicity assays, is a reliable correlate of extent of cytotoxicity with amyloid aggregation.

---

## **2. Materials**

1. Human wild-type (wt) synthetic A $\beta$ 42 and A $\beta$ 40 from a suitable commercial source (e.g., W.M. Keck Facility, Yale University, New Haven, CT, USA).
2. Trizma<sup>®</sup> hydrochloride solution (Tris-HCl) 1 M (Sigma, cat. no. T2663).
3. Uranyl acetate (UA) (Electron Microscopy Sciences, cat. no. 22400).
4. Formvar-coated TEM grids (Electron Microscopy Sciences, cat. no. FCF200-Cu-50).

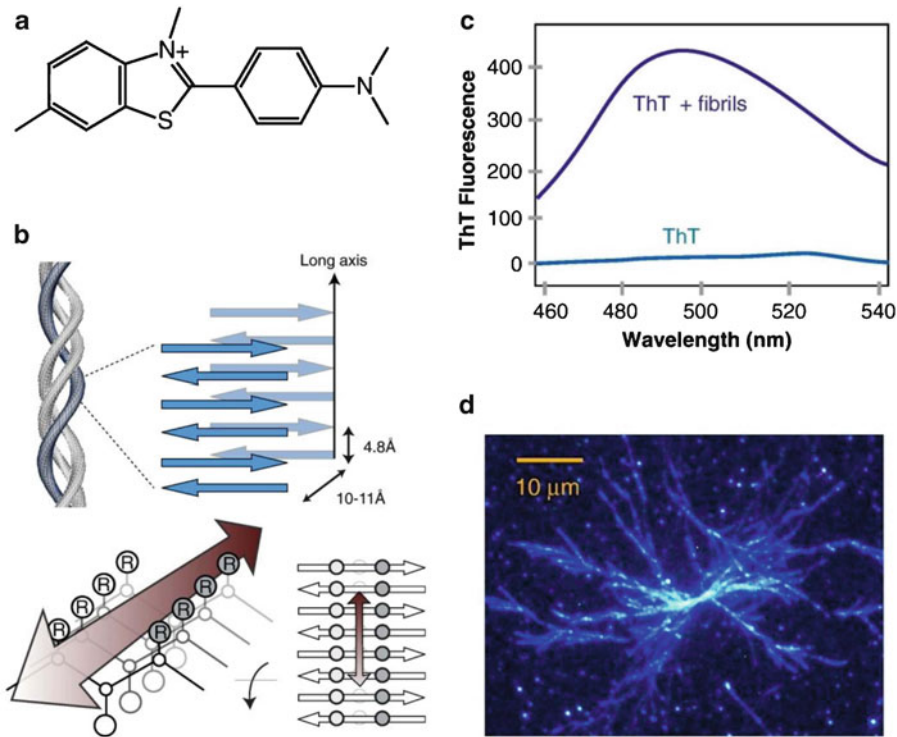


Fig. 4. Mechanism of ThT binding to the amyloid aggregates. (a) Structure of ThT. (b) Cross- $\beta$  structure of amyloid fibrils, formed from layers of laminated  $\beta$ -sheets. ThT is proposed to bind along surface side-chain grooves running parallel to the long axis of the  $\beta$ -sheet. (c) Characteristic increase in ThT fluorescence upon binding to amyloid fibrils. (d) TIRF microscopy image of branched glucagon fibrils stained with ThT (Images (a–c) are reprinted with copyright permission (41). The TIRF image (d) is reprinted with copyright permission (42)).

5. Grid storage box (Electron Microscopy Sciences, cat. no. 71140).
6. High Precision Ultrafine tweezers (Electron Microscopy Sciences, cat. no. 78318-3X).
7. Thioflavin-T (ThT) (Sigma, cat. no. T3516).
8. Glycine (Sigma, cat. no. 50046).
9. Sterile microtubes (e.g., Eppendorf cat. no. Z606340).
10. Dulbecco's Modified Eagle's Medium (DMEM) (Invitrogen, cat. no. 41966-029).
11. DMEM (Invitrogen, cat. no. 21063-029).
12. Recombinant insulin (Invitrogen, cat. no. 12585014).
13. Phosphate-buffered saline (PBS; GIBCO, cat. no. 10010-015).
14. Fetal bovine serum (FBS; GIBCO, cat. no. 10101145).
15. Penicillin–streptomycin (Pen–Strep, 100 $\times$ ; GIBCO, cat. no. 15140-122).
16. LDH cytotoxicity assay kit (Sigma, cat. no. TOX7).
17. MTT (3-(4,5-Dimethylthiazol-2-yl)-2,5-diphenyltetrazolium bromide) (Sigma, cat. no. M5655). Prepare 5 mg/ml MTT



stock solution in sterile PBS and filter through 0.22- $\mu$ m syringe-driven filter units (TPP, cat. no. 99722). The stock solution should be aliquoted in sterile microtubes (1 ml/tube) and frozen at  $-20^{\circ}\text{C}$ .

18. 96-Well, transparent bottom, cell culture plates (BD Falcon, cat. no. 353072).
19. 384-Well plates, black (Nunc, cat. no. 262260).
20. Dimethyl sulfoxide (DMSO) (Sigma, cat. no. D4540).
21. 1 N Hydrochloric acid solution (Sigma, cat. no. H9892).
22. Microplate reader (e.g., Safire 2, TECAN).
23. Poly-L-Lysine (PLL) 0.01% solution (Sigma, cat. no. P4832).
24. Rat pheochromocytoma (PC12) cells: PC12 cells are commercially available (e.g., ATCC, cat. no. CRL-1721) and should be grown in DMEM (Invitrogen, cat. no. 41966-029) supplemented with 1% Pen–Strep and 10% FBS (5% horse-serum, in addition to 10% FBS, during early passages) in 75-cm<sup>2</sup> culture flasks ( $37^{\circ}\text{C}$ ; ambient humidity; 5%  $\text{CO}_2$ ). It is recommended that the cells should be split before they reach complete confluence (twice/week), to record the number of passages and to keep some frozen stocks of the cells.

---

### 3. Methods

#### **3.1. Preparation of Crude A $\beta$ Preparations, Purified Monomers, Protofibrils, and Fibrils**

Detailed methods for the preparation and characterization of the crude A $\beta$  preparations, containing heterogeneous A $\beta$  aggregation states and monomers, or defined A $\beta$  species including monomers, protofibrils, and fibrils have been described previously (8, 21).

#### **3.2. Toxicity of A $\beta$ Preparations in PC12 Cell Cultures**

1. Plate PC12 cells in 96-well, transparent bottom, culture plates previously coated with 0.01% PLL (30,000 cells/well/200  $\mu$ l) in the culture medium consisting of phenol red-free DMEM medium (Invitrogen, cat. no. 21063-029) supplemented with 1% Pen–Strep and 2  $\mu$ M recombinant insulin. The cells should be grown in culture plates for at least 24 h ( $37^{\circ}\text{C}$ ; ambient humidity; 5%  $\text{CO}_2$ ), and should be treated with A $\beta$  preparation within 24–48 h after plating (see Note 1).
2. Dilute the A $\beta$  preparations (Subheading 3.1) in the culture medium at twice the final concentration(s) desired to be tested (see Note 2). For example, if the desired test A $\beta$  concentration is 10  $\mu$ M, dilute the A $\beta$  preparations to 20  $\mu$ M in appropriate volume of the culture medium.
3. Remove 100  $\mu$ l of the culture medium from each condition and control well and discard into a waste container.

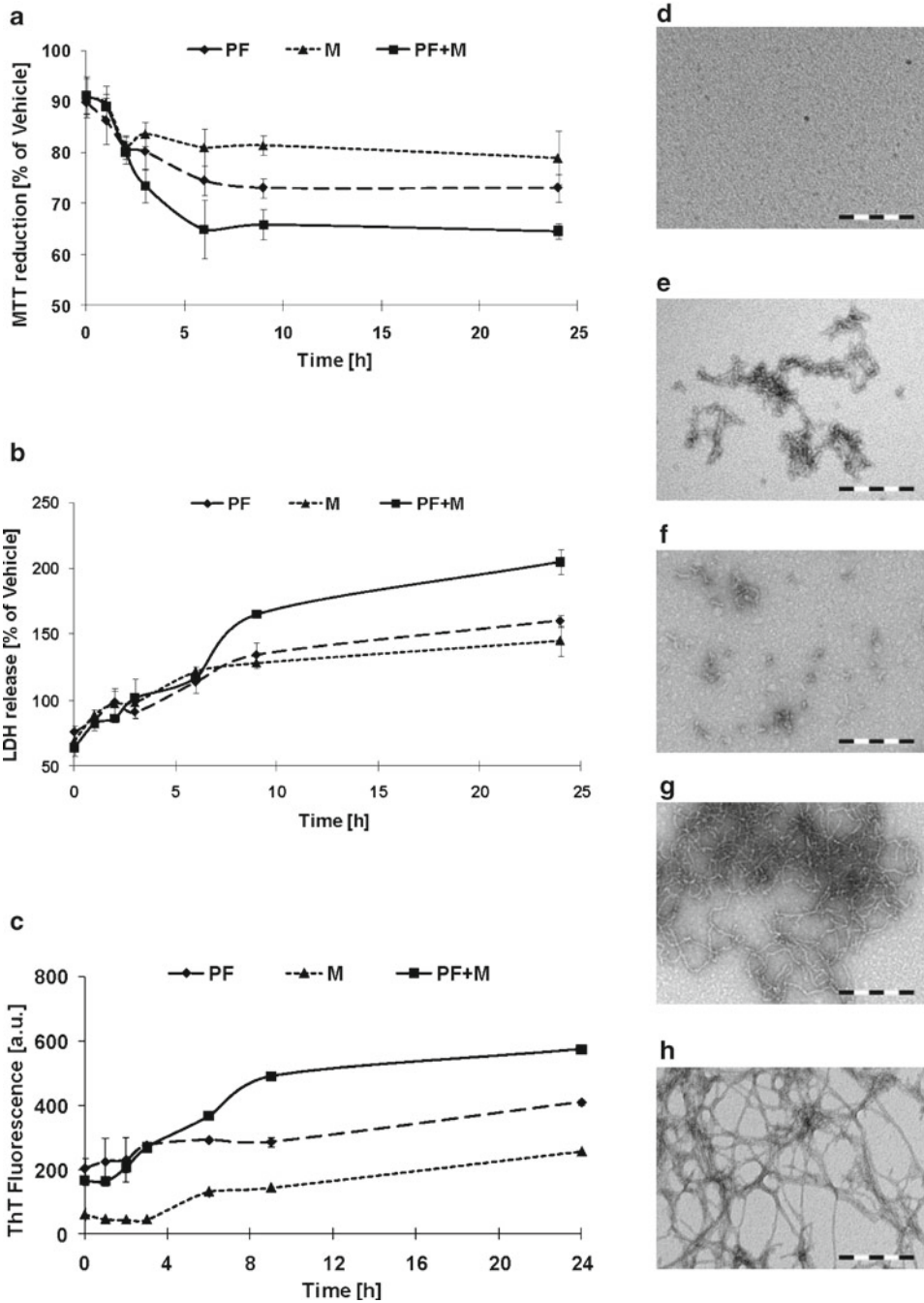


Fig. 5. Fibrillization and relative toxicities of the soluble Aβ42 preparations. Cultured PC12 cells were treated with purified Aβ42 preparations (*M* monomers, *PF* protofibrils, 1:1 molar mixtures of the monomers and protofibrils, i.e., 5 μM of each). The final Aβ concentration was ≈10 μM. (a) MTT reduction over time. Aβ42 protofibrils and mixtures of Aβ42 protofibrils with Aβ42 monomers significantly inhibit MTT reduction. In addition, the MTT reduction is significantly impaired with 6–9 h of Aβ42 treatment. The values are expressed as percentage of the buffer control (the error bars represent s.d. in at least six replicate conditions). (b) LDH release. Mixture of Aβ42 protofibrils and Aβ42 monomers cause early and robust increase in the LDH release as compared to the monomers, protofibrils, and fibrils alone. The values are expressed as percentage of the buffer control (the error bars represent s.d. in at least six replicate conditions). (c) ThT binding. Mixture of Aβ42 protofibrils and Aβ42 monomers fibrillize faster and to a greater extent than the monomers or protofibrils alone.

4. Add 100  $\mu$ l of culture medium containing A $\beta$  preparations, prepared in Subheading 3.2, step 2 to each condition well. To establish statistical significance, across different conditions and across different experiments, at least 4–6 wells should be treated with each A $\beta$  preparation.
5. Include medium only treated and buffer sample (prepared in identical fashion as the A $\beta$  preparations in step 2) treated cells as controls. If performing a time course study, the controls should be included for each time point.
6. At desired intervals (e.g., every hour), carefully remove 150  $\mu$ l of the culture medium, without touching the well bottom, into sterile microtubes and label accordingly. The removed medium will be used for assays outlined below (Subheadings 3.4–3.6).
7. Carefully remove the rest of the medium and discard.

### 3.3. MTT Reduction Assay

1. Wash the cells by adding 200  $\mu$ l of sterile PBS (room temperature) into each well and remove carefully without disturbing the cells in the bottom of the wells. Perform the PBS wash 2–3 times and discard into a waste container.
2. Add 100  $\mu$ l of the fresh culture medium containing 5% (vol./vol.) MTT dye solution to each well and place the cells back in the incubator for 2–4 h (see Note 3).
3. Carefully remove the culture medium and discard into a waste container. Then, add 100  $\mu$ l of the 100% DMSO to each well (see Note 3).
4. Solubilize the cells by careful pipetting and transfer the contents into empty wells of another 96-well plate. Transfer the latter plate to a 4°C chamber for storage not exceeding 24 h.
5. Repeat steps 1–4 above at each desired time point and collect the cell lysates. In order to avoid differential evaporation across the culture plates, add 200  $\mu$ l of sterile water to each empty well before placing the plate back in the incubator.
6. Warm the plate containing the cell lysate collected from each time point above, to 20–25°C [room temperature (RT)] by simply leaving the plate on a desk for 15 min.

---

Fig. 5. (continued) The *error bars* represent s.d. in at least six replicate conditions (a.u. = arbitrary units). (d–k) Representative images obtained by negative-staining TEM of the culture medium. (d, e) A $\beta$ 42 monomers at time 0 and 24 h respectively; (f, g) A $\beta$ 42 protofibrils at time 0 and 24 h respectively; (h) Equimolar mixtures of A $\beta$ 42 monomers and protofibrils and (k) A $\beta$ 40 monomers at 24 h (*scale bar* = 200 nm). These data show that an ongoing process of A $\beta$  oligomerization and fibrillization, rather than discrete A $\beta$  species (monomers, protofibrils, or fibrils), critically impairs cell viability (9, 10). In other words, dynamics of the protofibril–monomers interactions and the resultant growth of the protofibrils into fibrils is more important determinant of A $\beta$  toxicity than relatively stable protofibril species (8, 10). This hypothesis is also supported by the observations that enhancing the kinetic stability of A $\beta$ 42 protofibrils by adding A $\beta$ 40 monomers significantly reduces their toxicity toward cultured neurons (8). Similarly, small molecules that stabilize A $\beta$  protofibrils in vitro have also been shown to improve behavioral performance in APP transgenic mice (43).

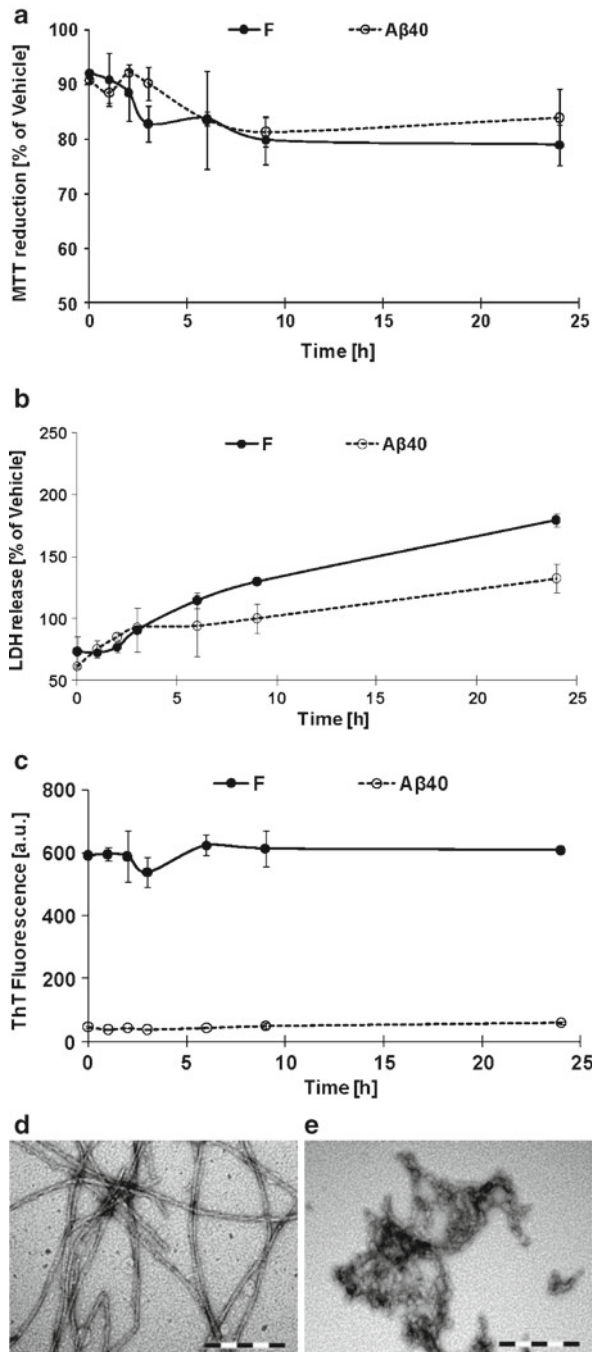


Fig. 6. Fibrillization and relative toxicities of A $\beta$ 40 monomers and A $\beta$ 42 fibrils. Cultured PC12 cells were treated with A $\beta$ 40 monomers and A $\beta$ 42 fibrils. The final A $\beta$  concentration was  $\approx 10 \mu\text{M}$ . **(a)** MTT reduction over time. Both A $\beta$ 40 monomers and A $\beta$ 42 fibrils cause slight, but insignificant, reduction in MTT metabolism by the cultured cells. The values are expressed as percentage of the buffer control (the *error bars* represent s.d. in at least six replicate conditions). **(b)** LDH release. A $\beta$ 42 fibrils cause relatively greater release of the cellular LDH as compared to A $\beta$ 40 monomers (the *error bars* represent s.d. in at least six replicate conditions). **(c)** ThT binding. The ThT binding by A $\beta$ 40 monomers remains relatively unchanged over time suggesting lack of fibril formation. The *error bars* represent s.d. in at least six replicate conditions (a.u. = arbitrary units). **(d, e)** Representative images obtained by negative-staining TEM of the culture medium. **(d)** A $\beta$ 42 fibrils and **(e)** A $\beta$ 40 after 24 h (scale bar = 200 nm).

7. Record the absorbance at 570 nm using a microplate reader. Use a wavelength in the range of 630–750 nm (e.g., 690 nm) as a reference wavelength to account for the plate background, cell debris, nonspecific absorbance etc.
8. Plot the data in a suitable software (Figs. 5a and 6a).

### **3.4. LDH Release Assay**

1. Prepare LDH assay mixture according to the manufacturer's recommendations (Sigma, cat. no. TOX7).
2. Vortex the tubes containing culture medium removed in Subheading 3.2, step 6 from each test and control condition.
3. Separately add 50  $\mu$ l of each test sample in empty wells of a transparent 96-well plate.
4. Add 100  $\mu$ l of the LDH assay mixture to each well.
5. Include the culture medium as a control sample.
6. Incubate the plate at 37°C for 20–30 min. Protect from light.
7. To stop the reaction, add 15  $\mu$ l of 1 N HCl to each well.
8. Record the absorbance at 490 nm using a microplate reader. Use a wavelength in the range of 630–750 nm (e.g., 690 nm) as a reference wavelength to account for the plate background, cell debris, nonspecific absorbance etc.
9. Plot the data in a suitable software (Figs. 5b and 6b).

### **3.5. Thioflavin-T Assay**

1. Vortex the tubes containing culture medium removed in Subheading 3.2, step 6 from each test and control condition.
2. Mix 80  $\mu$ l of the culture medium with 10  $\mu$ l of 100  $\mu$ M ThT (see Note 4) and 10  $\mu$ l of 500 mM glycine–NaOH pH 8.5 in corresponding wells of a Nunc 384 black well plate (see Note 5). Each sample should be assayed in at least duplicates.
3. Acquire ThT fluorescence values in a suitable fluorescence microplate reader using an excitation wavelength 450 nm and emission wavelength 485 nm (see Note 6).
4. Plot the data in a suitable software (see Figs. 5c and 6c).

### **3.6. Transmission Electron Microscopy**

1. Vortex the tubes containing culture medium removed in Subheading 3.2, step 6 from each test and control condition.
2. On a formvar-coated TEM grid, apply 2–10  $\mu$ l of one of the samples and let the droplet settle for ~60 s (see Note 7).
3. Then, using a blotting paper gently wick the edge of the sample grid and remove excess solution.
4. Apply a 10  $\mu$ l droplet of negative-staining solution (e.g., 2% wt/vol. UA) and let it settle for ~60 s on the grid surface (see Note 8).
5. Remove the excess solution as in step 3 above.

6. Using a fine vacuum probe, gently vacuum dry the grid from the edges. Sample grids not examined immediately can be stored in a storage box in a dry place (e.g., a desiccating chamber).
7. Acquire images on a CM10 TEM (or equivalent TEM), equipped with a CCD camera, operated at an acceleration voltage of 80–100 kV (Figs. 5d–h and 6d, e).

---

## 4. Notes

1. Other cell lines of neural origin (e.g., human neuroblastoma SHSY5Y cells) and/or primary neurons can be used as well. For culturing primary neurons, see the methods described elsewhere (21).
2. Excessive dilution of A $\beta$  samples can be avoided by preparing the A $\beta$  stock samples in supplemented 10 $\times$  DMEM (e.g., Sigma, cat. no. D2429) (10) or modified 100 $\times$  neurobasal medium (21).
3. Alternatively, commercially available kits can also be used with appropriate modifications to the procedure (e.g., Promega, cat. no. G4000).
4. A 100  $\mu$ M stock solution of ThT can be prepared as follows: Dissolve 0.32 mg of ThT in 10 ml of ultrapure H<sub>2</sub>O and vortex until a particulate-free solution is achieved. Filter the solution using a 0.22- $\mu$ m PES syringe filter. Aliquot the volume needed for the day (Subheading 3.5, step 2) and store the rest at 4°C. The solution can be stored at 4°C for 2–3 months. The presence of precipitates warrants immediate disposal. Protect from light by wrapping the tube in aluminum foil. To prepare 500 mM glycine–NaOH pH 8.5 solution, dissolve 376 mg of glycine in 10 ml of ultrapure H<sub>2</sub>O until clear. Bring the pH to 8.5 by drop by drop addition of 1 N NaOH and continuous mixing. Filter the solution with a 0.22- $\mu$ m PES syringe filter and store at 4°C. Remove the volume needed for the day (Subheading 3.5, step 2), and store the rest at 4°C for up to 2–3 months. Presence of precipitates warrants immediate disposal.
5. The described step is optimized for final concentration of A $\beta$   $\leq$  10  $\mu$ M, ThT:A $\beta$  ratio  $\geq$  1 and final glycine–NaOH concentration being 50 mM. The step can be modified to accommodate different concentrations of A $\beta$ . For example: For a sample of 50  $\mu$ M A $\beta$ , either dilute the sample with normal culture medium to 10  $\mu$ M and proceed as above or use 70 mM glycine–NaOH stock solution (20  $\mu$ l A $\beta$  + 70  $\mu$ l glycine–NaOH + 10  $\mu$ l ThT (100  $\mu$ M)).

6. In addition to the excitation and emission wavelengths, adjust the settings of the fluorometer as follows: (1) number of reads (5–10); (2) plate (Nunc 384-well black); (3) Z-height (middle of the well); (4) integration time (100 ms); and (5) reading interval (10  $\times$  10 ms).
7. To reduce the TEM grid surface contamination and hydrophobicity, it is recommended to apply the glow discharge the grids prior to the sample application.
8. A 2% wt/vol. UA stock solution can be prepared as follows: Dissolve 200 mg of UA in 10 ml of ultrapure H<sub>2</sub>O and vortex until a particulate-free solution is achieved. Filter the solution using a syringe-driven 0.22- $\mu$ m PES filter and store at 4°C. The solution should be prepared as needed and can be stored at 4°C for 1 month. Dispose of the solution as per institutional regulations. Wear gloves while handling.

---

## Acknowledgments

This work was supported by the Swiss Federal Institute of Technology Lausanne (EPFL) and grants from the Swiss National Foundation (Grant# 310000-110027). The authors thank AC Immune (S.A.), Lausanne, Switzerland for financially supporting Asad Jan. We also thank Prof. Andrea Pfeifer, Dr. Andreas Muhs, and Dr. Oskar Adolfsson from AC Immune (S.A.), Lausanne Switzerland for thoughtful discussions.

## References

1. Selkoe, D. J. (1991) Amyloid protein and Alzheimer's disease, *Sci.Am.* **265**, 68–66, 78.
2. Hardy, J. A., and Higgins, G. A. (1992) Alzheimer's disease: the amyloid cascade hypothesis, *Science* **256**, 184–185.
3. Selkoe, D. J. (2001) Alzheimer's disease: genes, proteins, and therapy, *Physiol Rev* **81**, 741–766.
4. Walsh, D. M., Lomakin, A., Benedek, G. B., Condron, M. M., and Teplow, D. B. (1997) Amyloid beta-protein fibrillogenesis. Detection of a protofibrillar intermediate, *J Biol Chem* **272**, 22364–22372.
5. Lambert, M. P., Barlow, A. K., Chromy, B. A., Edwards, C., Freed, R., Liosatos, M., Morgan, T. E., Rozovsky, I., Trommer, B., Viola, K. L., Wals, P., Zhang, C., Finch, C. E., Krafft, G. A., and Klein, W. L. (1998) Diffusible, nonfibrillar ligands derived from Abeta1–42 are potent central nervous system neurotoxins, *Proc.Natl.Acad.Sci.U.S.A* **95**, 6448–6453.
6. Lashuel, H. A., Hartley, D. M., Petre, B. M., Wall, J. S., Simon, M. N., Walz, T., and Lansbury, P. T., Jr. (2003) Mixtures of wild-type and a pathogenic (E22G) form of Abeta40 in vitro accumulate protofibrils, including amyloid pores, *J.Mol.Biol.* **332**, 795–808.
7. Bitan, G., Kirkitadze, M. D., Lomakin, A., Vollers, S. S., Benedek, G. B., and Teplow, D. B. (2003) Amyloid beta -protein (Abeta) assembly: Abeta 40 and Abeta 42 oligomerize through distinct pathways, *Proc.Natl.Acad.Sci. USA* **100**, 330–335.
8. Jan, A., Gokce, O., Luthi-Carter, R., and Lashuel, H. A. (2008) The ratio of monomeric to aggregated forms of Abeta40 and Abeta42 is an important determinant of amyloid-beta aggregation, fibrillogenesis, and toxicity, *J Biol Chem* **283**, 28176–28189.
9. Wogulis, M., Wright, S., Cunningham, D., Chilcote, T., Powell, K., and Rydel, R. E. (2005) Nucleation-dependent polymerization is an

- essential component of amyloid-mediated neuronal cell death, *J Neurosci* **25**, 1071–1080.
10. Jan, A., Adolfsson, O., Allaman, I., Buccarello, A. L., Magistretti, P. J., Pfeifer, A., Muhs, A., and Lashuel, H. A. (2010) A[ $\beta$ ]<sub>42</sub> neurotoxicity is mediated by ongoing nucleated polymerization process rather than by discrete A[ $\beta$ ]<sub>42</sub> species, *J Biol Chem* **286**, 8585–8596.
  11. Lemere, C. A., Blusztajn, J. K., Yamaguchi, H., Wisniewski, T., Saido, T. C., and Selkoe, D. J. (1996) Sequence of deposition of heterogeneous amyloid beta-peptides and APO E in Down syndrome: implications for initial events in amyloid plaque formation, *Neurobiol Dis* **3**, 16–32.
  12. McLean, C. A., Cherny, R. A., Fraser, F. W., Fuller, S. J., Smith, M. J., Beyreuther, K., Bush, A. I., and Masters, C. L. (1999) Soluble pool of Abeta amyloid as a determinant of severity of neurodegeneration in Alzheimer's disease, *Ann. Neurol.* **46**, 860–866.
  13. Moechars, D., Dewachter, I., Lorent, K., Reverse, D., Baekelandt, V., Naidu, A., Tesseur, I., Spittaels, K., Haute, C. V., Checler, F., Godaux, E., Cordell, B., and Van Leuven, F. (1999) Early phenotypic changes in transgenic mice that overexpress different mutants of amyloid precursor protein in brain, *J Biol Chem* **274**, 6483–6492.
  14. Holcomb, L., Gordon, M. N., McGowan, E., Yu, X., Benkovic, S., Jantzen, P., Wright, K., Saad, I., Mueller, R., Morgan, D., Sanders, S., Zehr, C., O'Campo, K., Hardy, J., Prada, C. M., Eckman, C., Younkin, S., Hsiao, K., and Duff, K. (1998) Accelerated Alzheimer-type phenotype in transgenic mice carrying both mutant amyloid precursor protein and presenilin 1 transgenes, *Nat. Med.* **4**, 97–100.
  15. Walsh, D. M., Klyubin, I., Fadeeva, J. V., Cullen, W. K., Anwyl, R., Wolfe, M. S., Rowan, M. J., and Selkoe, D. J. (2002) Naturally secreted oligomers of amyloid beta protein potently inhibit hippocampal long-term potentiation in vivo, *Nature* **416**, 535–539.
  16. Nilsberth, C., Westlind-Danielsson, A., Eckman, C. B., Condron, M. M., Axelman, K., Forsell, C., Sten, C., Luthman, J., Teplow, D. B., Younkin, S. G., Naslund, J., and Lannfelt, L. (2001) The 'Arctic' APP mutation (E693G) causes Alzheimer's disease by enhanced Abeta protofibril formation, *Nat Neurosci* **4**, 887–893.
  17. Walsh, D. M., Hartley, D. M., Kusumoto, Y., Fezoui, Y., Condron, M. M., Lomakin, A., Benedek, G. B., Selkoe, D. J., and Teplow, D. B. (1999) Amyloid beta-protein fibrillogenesis. Structure and biological activity of protofibrillar intermediates, *J. Biol. Chem.* **274**, 25945–25952.
  18. Hartley, D. M., Walsh, D. M., Ye, C. P., Diehl, T., Vasquez, S., Vassilev, P. M., Teplow, D. B., and Selkoe, D. J. (1999) Protofibrillar intermediates of amyloid beta-protein induce acute electrophysiological changes and progressive neurotoxicity in cortical neurons, *J. Neurosci.* **19**, 8876–8884.
  19. Whalen, B. M., Selkoe, D. J., and Hartley, D. M. (2005) Small non-fibrillar assemblies of amyloid beta-protein bearing the Arctic mutation induce rapid neurotoxic degeneration, *Neurobiol Dis* **20**, 254–266.
  20. Mucke, L. (2009) Neuroscience: Alzheimer's disease, *Nature* **461**, 895–897.
  21. Jan, A., Hartley, D. M., and Lashuel, H. A. (2010) Preparation and characterization of toxic A[ $\beta$ ] aggregates for structural and functional studies in Alzheimer's disease research, *Nat. Protocols* **5**, 1186–1209.
  22. Mosmann, T. (1983) Rapid colorimetric assay for cellular growth and survival: application to proliferation and cytotoxicity assays, *J Immunol Methods* **65**, 55–63.
  23. Berridge, M. V., Herst, P. M., and Tan, A. S. (2005) Tetrazolium dyes as tools in cell biology: new insights into their cellular reduction, *Biotechnol Annu Rev* **11**, 127–152.
  24. Wu, B., Zhu, J. S., Zhang, Y., Shen, W. M., and Zhang, Q. (2008) Predictive value of MTT assay as an in vitro chemosensitivity testing for gastric cancer: one institution's experience, *World J Gastroenterol* **14**, 3064–3068.
  25. Mueller, H., Kassack, M. U., and Wiese, M. (2004) Comparison of the usefulness of the MTT, ATP, and calcein assays to predict the potency of cytotoxic agents in various human cancer cell lines, *J Biomol Screen* **9**, 506–515.
  26. Chromy, B. A., Nowak, R. J., Lambert, M. P., Viola, K. L., Chang, L., Velasco, P. T., Jones, B. W., Fernandez, S. J., Lacor, P. N., Horowitz, P., Finch, C. E., Krafft, G. A., and Klein, W. L. (2003) Self-assembly of Abeta(1–42) into globular neurotoxins, *Biochemistry* **42**, 12749–12760.
  27. Green, P. S., Perez, E. J., Calloway, T., and Simpkins, J. W. (2000) Estradiol attenuation of beta-amyloid-induced toxicity: a comparison o, *J Neurocytol* **29**, 419–423.
  28. Janjic, D., and Wollheim, C. B. (1992) Islet cell metabolism is reflected by the MTT (tetrazolium) colorimetric assay, *Diabetologia* **35**, 482–485.
  29. Decker, T., and Lohmann-Matthes, M. L. (1988) A quick and simple method for the quantitation of lactate dehydrogenase release in measurements of cellular cytotoxicity and tumor necrosis factor (TNF) activity, *J Immunol Methods* **115**, 61–69.



30. Lappalainen, K., Jaaskelainen, I., Syrjanen, K., Urtti, A., and Syrjanen, S. (1994) Comparison of cell proliferation and toxicity assays using two cationic liposomes, *Pharm Res* **11**, 1127–1131.
31. Jurisic, V. (2003) Estimation of cell membrane alteration after drug treatment by LDH release, *Blood* **101**, 2894; author reply 2895.
32. Kehrer, G., Blech, M., Kallerhoff, M., and Bretschneider, H. J. (1989) Urinary LDH-release for evaluation of postischemic renal function, *Klin Wochenschr* **67**, 477–485.
33. Lobner, D. (2000) Comparison of the LDH and MTT assays for quantifying cell death: validity for neuronal apoptosis?, *J Neurosci Methods* **96**, 147–152.
34. Legrand, C., Bour, J. M., Jacob, C., Capiamont, J., Martial, A., Marc, A., Wudtke, M., Kretzmer, G., Demangel, C., Duval, D., and et al. (1992) Lactate dehydrogenase (LDH) activity of the cultured eukaryotic cells as marker of the number of dead cells in the medium [corrected], *J Biotechnol* **25**, 231–243.
35. Terry, R. D., Gonatas, N. K., and Weiss, M. (1964) Ultrastructural Studies in Alzheimer's Presenile Dementia, *Am J Pathol* **44**, 269–297.
36. Haass, C., and Selkoe, D. J. (2007) Soluble protein oligomers in neurodegeneration: lessons from the Alzheimer's amyloid beta-peptide, *Nat Rev Mol Cell Biol* **8**, 101–112.
37. Lashuel, H. A., and Wall, J. S. (2005) Molecular electron microscopy approaches to elucidating the mechanisms of protein fibrillogenesis, *Methods Mol Biol* **299**, 81–101.
38. Maezawa, I., Hong, H. S., Liu, R., Wu, C. Y., Cheng, R. H., Kung, M. P., Kung, H. F., Lam, K. S., Oddo, S., Laferla, F. M., and Jin, L. W. (2008) Congo red and thioflavin-T analogs detect Abeta oligomers, *J Neurochem* **104**, 457–468.
39. Yamamoto, T., and Hirano, A. (1986) A comparative study of modified Bielschowsky, Bodian and thioflavin S stains on Alzheimer's neurofibrillary tangles, *Neuropathol Appl Neurobiol* **12**, 3–9.
40. Uversky, V. N., Li, J., Souillac, P., Millett, I. S., Doniach, S., Jakes, R., Goedert, M., and Fink, A. L. (2002) Biophysical properties of the synucleins and their propensities to fibrillate: inhibition of alpha-synuclein assembly by beta- and gamma-synucleins, *J Biol Chem* **277**, 11970–11978.
41. Biancalana, M., and Koide, S. (2010) Molecular mechanism of Thioflavin-T binding to amyloid fibrils, *Biochim Biophys Acta* **1804**, 1405–1412.
42. Andersen, C. B., Yagi, H., Manno, M., Martorana, V., Ban, T., Christiansen, G., Otzen, D. E., Goto, Y., and Rischel, C. (2009) Branching in amyloid fibril growth, *Biophys J* **96**, 1529–1536.
43. Hawkes, C. A., Deng, L. H., Shaw, J. E., Nitz, M., and McLaurin, J. (2010) Small molecule beta-amyloid inhibitors that stabilize protofibrillar structures in vitro improve cognition and pathology in a mouse model of Alzheimer's disease, *Eur J Neurosci* **31**, 203–213.